Copyright © 2009 Tech Science Press SDHM, vol.5, no.2, pp.87-107, 2009

Temperature Sensitivity Assessment of Vibration-based Damage Identification Techniques

N.H.M. Kamrujjaman Serker[1] **and Zhishen Wu**

Abstract: This paper presents the study on the temperature sensitivity of some vibration-based damage identification techniques. With the help of a simple supported beam with different damage levels, reliability of these techniques for damage identification in a changing environmental temperature condition was investigated. The temperature effect was considered as the change in modulus of elasticity of the material. The techniques evaluated herein are based on measured modal parameters which use only few mode shapes and/or modal frequencies of the structure that can easily be obtained by dynamic tests. The effect of temperature on identification of different level of damages at different locations was evaluated. The studied results show that both damage localization and quantification can be affected in presence of the temperature effect which can lead the damage detection unreliable. Among the studied methods, frequency based damage detection method and change in flexibility method are found to be more sensitive to the temperature effect.

Keywords: Damage Identification, Temperature Effect, Vibration Test, Modal Parameters

1 Introduction

For the last few decades, vibration tests on civil engineering structures are being performed to identify and localize damage. Several methods have been proposed for these purposes considering the changes in vibration features extracted from the vibration measurements. For example, damages may be characterized by changes in the modal parameters, i.e., natural frequencies, modal damping ratios and mode shapes. A detailed review on this research topic is available in Doebling *et al.* (1996) and Montalovao *et al.* (2006). A summary of some vibration based dam-

[1] Department of Urban & Civil Engineering, Ibaraki University 4-12-1 NakaNarusawa, Hitachi, Ibaraki, Japan 316-0036. Tel: +81 294 38 5247; Fax: +81 294 38 5268; E-mail: kserker@gmail.com

age identification methods is also added to this paper. In most of the previous studies, vibration characteristics of structures were estimated with the assumption of a constant environmental condition. However, in practical situations, structures often experience varying environmental and operational conditions (e.g., temperature, temperature gradients, humidity, wind, traffic, etc.). It became more and more clear that environmental parameters affect the dynamic behavior of a structure. For example, the Young's modulus of concrete decreases with increasing temperature which in turn causes drop in natural frequencies of the structure. These varying environmental conditions may mask or magnify the changes in the modal parameters caused by structural damages. False-positive or negative damage diagnosis may occur if the effect of the environmental variations is not taken into account in the damage detection process which may cause the vibration-based damage identification unreliable and during the last years, researchers have become increasingly concerned with modal parameter variability due to environmental conditions (Yan *et al.*,2005). For example, Wahab and De Roeck (1997) observed on a prestressed concrete highway bridge that the temperature can change the natural frequencies of all modes by 4-5% without changing the mode shapes significantly. Cornwell *et al.* (1999) measured the frequencies of the Alamosa Canyon Bridge in different environmental condition and concluded that the frequencies of the 1st, 2nd and 3rd modes varied by 4.7%, 6.6% and 5%, respectively over the 24-hour period. Lloyd *et al.* (2000) measured the modal frequencies of a long span pre-stressed concrete bridge for a seven months period with an environmental temperature ranged between -15°C to 33°C. The measured data showed that the frequencies vary linearly for the first few modes in an order of 2 x 10^{-3} to 3 x 10^{-3} Hz/°C. Xia *et al.* (2006) tested a concrete slab and observed that the modal frequencies decrease by 0.13 - 0.23% when temperature increases by one degree Celsius or decrease by 0.03% when relative humidity increases by 1%. Since the modal parameters can be changed under the environmental temperature variations, damage identification methods may lead to erroneous results in such conditions. Therefore, there is a need for the evaluation of the damage identification methods under the environmental temperature effect on the structures to be examined or monitored. This paper presents the evaluation of some vibration based damage identification methods with the temperature effect. Numerical case studies on a beam-like structure were carried out to evaluate the performance of the selected damage identification algorithms.

2 Summary of the vibration-based damage identification algorithms

Several vibration based damage identification algorithms based on the mode shapes and frequency change were evaluated in this study. A brief introduction of the damage identification methods is given here.

2.1 Frequency Based Damage Detection (FBDD)

Kim *et al.* (2003) presented a damage indicator based on the measured frequency changes of the structure as

$$DI_j = \left[\sum_{i=1}^{NM} e_{ij}^2\right]^{-1/2} \tag{1}$$

in which e_{ij} is an error index defined as

$$e_{ij} = Z_i / \sum_{k=1}^{NM} Z_k - F_{ij} / \sum_{k=1}^{NM} F_{kj} \tag{2}$$

where Z_i/Z_k is the ratio of the fractional change in i^{th} eigen value to the fractional change in k^{th} eigen value. F_{ij}/F_{kj} is the ratio of sensitivity for i^{th} ode and j^{th} element to the sensitivity of k^{th} mode and j^{th} element. NM is the number of modes. Maximum value of the error index indicates the presence of damage at that location.

2.2 Mode Shape Curvature based Damage Identification Method

2.2.1 Mode Shape Curvature Method (MSC)

Pandey *et al.* (1991) first proposed the MSC method by using the central difference approximation as

$$\phi_{ij}'' = \frac{\phi_{(i+1)j} - 2\phi_{ij} + \phi_{(i-1)j}}{h^2} \tag{3}$$

Here, h is the distance between the measurement locations and ϕ_{ij} are the modal displacements of mode shape j at the measurement location i. The location of the damage is assessed by the largest computed absolute difference between the mode shape curvature of the damaged and undamaged structure as follows:

$$\Delta\phi_{ij}'' = \left|\phi_{ij}^{*\prime\prime} - \phi_{ij}''\right|. \tag{4}$$

where ϕ_{ij}'' and $\phi_{ij}^{*\prime\prime}$ are the mode shape curvature of undamaged and damaged structure respectively. $\Delta\phi_{ij}''$ is the absolute change in mode shape curvature between the damage and undamaged structures. If more than one mode is used, the index is given by

$$MSC_i = \sum_j \Delta\phi_{ij}''. \tag{5}$$

2.2.2 Mode Shape Curvature based Damage Index Method (MSCDI)

This method is also known as the damage index method, developed by Stubbs *et al.* (1995), also makes use of the mode shape curvature changes. It is defined by

$$\beta_{ij} = \frac{\left(\int_a^b \left[\phi''^*_j(x)\right]^2 dx + \int_0^L \left[\phi''^*_j(x)\right]^2 dx\right) \int_a^b \left[\phi''_j(x)\right]^2 dx}{\left(\int_a^b \left[\phi''_j(x)\right]^2 dx + \int_0^L \left[\phi''_j(x)\right]^2 dx\right) \int_a^b \left[\phi^{*''}_j(x)\right]^2 dx} \tag{6}$$

where a and b are the limits of a segment i of the beam where damage is being evaluated and L is the total length of the same beam. ϕ'' and j have the same meaning as given in Eqn. (3) and (4). For more than one mode, the damage index can be defined as

$$DI_i = \sum_j \beta_{ij} \tag{7}$$

2.3 Dynamically Measured Flexibility-based Damage Detection Methods

2.3.1 Change in Flexibility Method

Another class of damage identification methods uses the dynamically measured flexibility matrix to estimate changes in the static behavior of the structure (Pandey and Biswas, 1994). The expression of the flexibility matrix is written as

$$F = \sum_{i=1}^{n} \frac{1}{\omega_i^2} \phi_i \phi_i^T \tag{8}$$

and the change in flexibility matrix can be obtained as

$$\Delta = F^* - F \tag{9}$$

where ϕ_i is the i^{th} mode shape, $\omega_i$is the i^{th} modal frequency, n is the number of measured mode shapes, F and F* are, respectively, flexibility matrices before and after damage and Δ is the flexibility variation matrix. The damage index is defined as

$$\bar{\delta}_j = \max\left|\delta_{ij}\right| \tag{10}$$

where δ_{ij} are elements of matrix Δ and $\bar{\delta}_j$ is the absolute maximum of the elements in the j^{th} column.

2.3.2 Change in Flexibility Curvature Method (FCM)

By combining certain aspects of the mode shape curvature method and the change in flexibility method, Zhang and Aktan (1995) developed an alternative damage detection scheme known as change in flexibility curvature method. The basic concept is similar to the mode shape curvature method that a localized loss of stiffness will produce a curvature increase at the same location. However, the change in curvature is obtained from the flexibility instead of curvature. The flexibility curvature change is evaluated as follows:

$$\left[\Delta F''\right] = \sum_{i=1}^{n} \left|[F_i^*]'' - [F_i]''\right| \tag{11}$$

where $[\Delta F'']$ and n represent, respectively, the absolute curvature changes and the number of identified mode shapes. $[F]''$ and $[F]''$ are, respectively, flexibility curvature matrices before and after damage. The elements of $[\Delta F'']$ that have comparatively large values correspond to damage location.

2.4 Modal Macro Strain Vector (MMSV) based Damage Index Method

Li and Wu (2007) proposed the MMSV based damage index for the identification and localization of the damage with the application of distributed strain sensing technique. The damage index is defined by

$$\beta_{mr} = \frac{\psi_{mr}^* - \psi_{mr}}{\psi_{mr}} \times 100 \tag{12}$$

where ψ_{mr} and ψ_{mr}^*, respectively the component of the normalized MMSV before and after damage and is defined as

$$\{\psi_{1r}, \psi_{2r}, \ldots \psi_{mr}, \ldots..\} = \left\{\frac{\delta_{1r}}{\delta_{br}}, \frac{\delta_{2r}}{\delta_{br}}, \ldots\ldots \frac{\delta_{mr}}{\delta_{br}} \ldots..\right\} \tag{13}$$

whereδ_{mr}, is the modal macro strain of the m^{th} location and for the r^{th} mode and δ_{br} is the reference modal macro strain for the r^{th} mode.

3 Temperature effects on modal frequency

For a simply supported uniform beam of length L, height H, density ρ and modulus of elasticity E, its undamped flexural vibration frequency of order $n$is (Clough and Penzien, 1993)

$$f_n = \frac{n^2 \pi h}{2l^2} \sqrt{\frac{E}{12\rho}} \tag{14}$$

Temperature change has various effects on the structure such as change in the value of elastic modulus of the materials, change in geometry, thermal expansion or contraction. Variations of the elastic modulus of structure materials can be written as a function of temperature based on its rates of change around a reference temperature as:

$$E(T) = E_0(1+\alpha_E \Delta T) \tag{15}$$

where E is the Yong's modulus at the measuring temperature, E_0 is the elastic modulus at the reference temperature and α_E is the linear change in Young's modulus with respect to temperature.

For a small change in temperature, the coefficient of linear thermal expansion, α_T, can be considered approximately constant. Therefore, the structural dimensions can be written as function of temperature

$$B = B_0\,(1+\alpha_T \Delta T), \quad L = L_0\,(1+\alpha_T \Delta T), \quad H = H_0\,(1+\alpha_T \Delta T) \tag{16}$$

where B is the width. B_0, L_0 and H_0 are respectively the width, length and thickness of the beam at reference temperature.

Due to the thermal expansion, the beam density per unit volume also varies with temperature and can be expressed as

$$\rho = \frac{M}{V} = \frac{M}{B_0 L_0 H_0 (1+\alpha_T \Delta T)^3} = \frac{M}{V_0 (1+\alpha_T \Delta T)^3} = \frac{\rho_0}{(1+\alpha_T \Delta T)^3} \tag{17}$$

where M is the mass of the beam, ρ is the mass density of the beam and ρ_0 is the mass density of the beam at the reference temperature. V_0 is the volume of the beam at the reference temperature.

Substituting Eqn. (15) and (17) into Eqn. (14)

$$f_n = \frac{n^2 \pi H_0}{2L_0^2} \sqrt{\frac{E_0\,(1+\alpha_E \Delta T)\,(1+\alpha_T \Delta T)}{12\rho_0}} \tag{18}$$

Eqn. (18) estimates the rate of frequency change with temperature change. For steel, α_E is about 3.6 $\times$ 10^{-4}/C and α_t is about 1.1 $\times$ 10^{-5}/C at 25C (Brockenbrough and Merritt, 1994). For concrete, α_t is about 1.0 $\times$ 10^{-5}/°C. There is very little published data for α_E of concrete in the ambient temperature range. Baldwin and Nordich (1978) showed that the modulus of elasticity of concrete decreases approximately linearly with temperature and the coefficient α_E is about -4.5 x 10^{-3} /°C for t < 100°C and -1.4 x 10^{-3} /°C for t > 100°C. Obviously α_E of steel and concrete is much higher than α_t. Therefore, variation of Young's modulus with temperature is much more significant than thermal expansion.

4 Numerical studies on beam-like structure

A simple beam-like structure, shown in Figure 1, was considered in this numerical simulation study. It is obvious that the temperature change has various effects on the structure such as change in the value of elastic modulus of the materials, change in geometry, thermal expansion or contraction. In previous section, it is shown that the effect of variation of Young's modulus with temperature is much more significant than the effect of thermal expansion. Therefore, the effect of the temperature variation on the geometry of the structure is not considered in this study. Due to the lacking of temperature dependent material models in the ambient temperature range, temperature effect was indirectly simulated by considering a reduction in the elastic modulus of the structural material as the equivalent temperature change. A uniform temperature change over the whole beam was applied. 1% reduction in modulus of elasticity was considered to consider the nominal environmental temperature effect. Such amount of reduction in elastic modulus is equivalent to the reduction in elastic modulus due to an approximate change in temperature of 30°C. Structural damage was considered as the reduction in flexural rigidity of the corresponding section of the beam. Modal analysis was performed with the commercial finite element analysis software, ANSYS, and 2D beam element with two d.o.f. at each intermediate node, a vertical translation and a rotation, was chosen for this study. The FE model and the details of the beam are given in Figure 1.

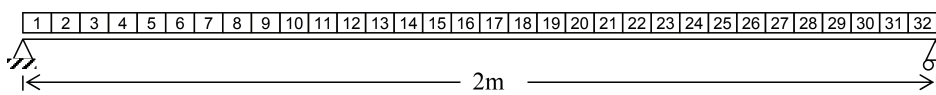

E= 2.1×10^{11} N/m^2; B=0.03m; H= 0.01m; ρ= 7830 kg/m^3

Figure 1: Finite element model of the beam

4.1 Damage Scenarios

Damage scenarios listed in Table 1 were considered in this study. In flexible structures, damage are likely to occur at or near the midspan. Therefore, damage was applied separately to elements, 12 and 16. Another damage scenario was considered to study the effect of temperature on damage location by considering damage at element 8. By selecting such damage locations, sensitivity of different algorithms to the temperature variation in damage detection at different location can be assessed as well.

Table 1: Description of the damage cases

Description	Damage Case No.		
	Damage at Element 8	Damage at Element 12	Damage at Element 16
5% Damage only	C1	C9	C17
5% Damage with Temperature Effect	C2	C10	C18
10% Damage only	C3	C11	C19
10% Damage with Temperature Effect	C4	C12	C20
30% Damage only	C5	C13	C21
30% Damage with Temperature Effect	C6	C14	C22
50% Damage only	C7	C15	C23
50% Damage with Temperature Effect	C8	C16	C24

5 Numerical analyses results

In this section, results of the simulation case studies are presented. At first, temperature effect on the change of natural frequency of different modes was examined. First five flexural modes of the studied beam-like structure were considered in this study. Selected mode shapes were verified using the Modal Assurance Criteria (MAC) to check their identicalness. Finally, different damage identification algorithms were used to identify, localize and quantify different level of damage at different location along the beam.

5.1 Effect of Damage and Temperature on Natural Frequencies

First five natural frequencies of the intact structure along with the effect of temperature only are listed in Table 2. Percentage change in natural frequencies of the first five modes for different level of damages with and without the effect of temperature at different locations is shown in Figure 2. The numerical study results show that drop in natural frequencies is affected significantly under the influence of temperature effect. From Table 2 and Figure 2 it is obvious that the percentage change in frequencies of all modes of the intact structure due to the temperature effect is much higher than that due to a single damage with a reduction in stiffness up to 10%. At other damage levels, magnification of the drop in frequency due to temperature effect can easily be noticed.

(a)

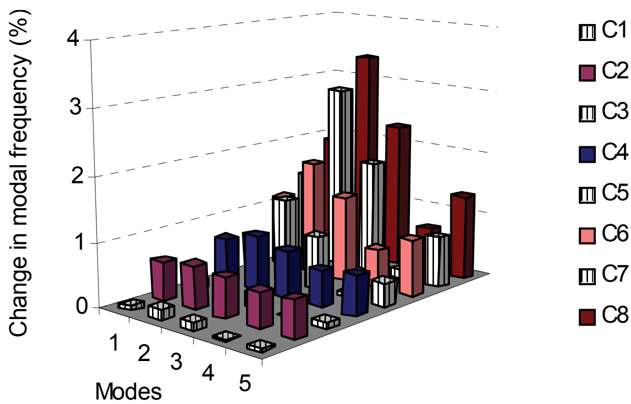

(b)

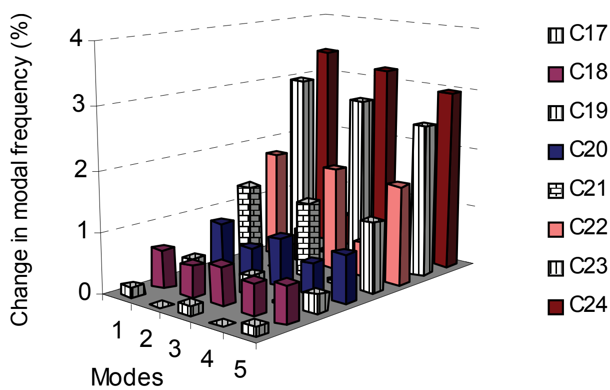

(c)

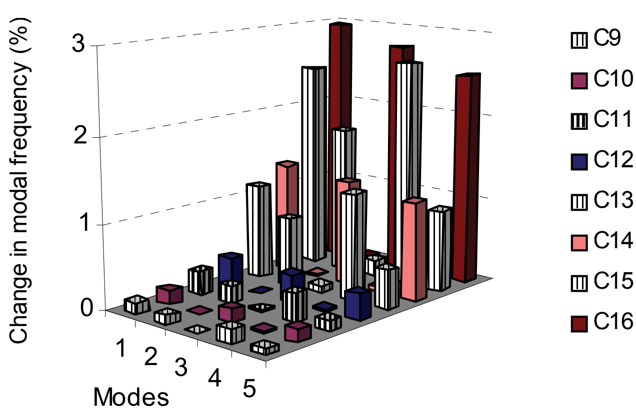

Figure 2: Effect of temperature on modal frequency (a) damage at element 8 (b) damage at element 12 (c) damage at element 16

Table 2: Effect of temperature on frequencies of the intact beam

Mode no.	Natural frequencies (Hz)		Percentage change in frequency
	Without Temperature effect	With Temperature Effect	
1	5.83	5.80	0.56
2	23.31	23.19	0.56
3	52.43	52.17	0.56
4	93.21	92.74	0.56
5	145.63	144.89	0.56

5.2 Variation in Modeshapes due to Temperature Effect

MAC value was used to quantify the variation in mode shapes. The MAC value is defined as (Ewins, 2000)

$$MAC\left(\left\{\phi_i^A\right\},\left\{\phi_i^E\right\}\right)=\frac{\left|\left\{\phi_i^A\right\}^T\left\{\phi_i^E\right\}\right|^2}{\left(\left\{\phi_i^A\right\}^T\left\{\phi_i^A\right\}\right)\left(\left\{\phi_i^E\right\}^T\left\{\phi_i^E\right\}\right)} \tag{19}$$

where ϕ_i is the i^{th} mode shape, superscript "A" and "E" represent intact and damaged, respectively. In the case where the two mode shapes are identical the MAC value would be equal to unity. Any variation in the mode shapes would generate a MAC value less than unity, and it decreases to zero when there is no correlation. Here, mode shapes of the undamaged structure were employed as a baseline. The MAC values of the first five modes with respect to 5% damage at element 12 without and with temperature effect are shown in Tables 3 and 4 respectively. All the diagonal entries in both of the tables are equal to or nearly equal to 1. Therefore, the effect of the temperature on mode shapes was not significant. Some changes in the values of the off-diagonal entries of Tables 3 and 4 were noticed. These changes may be resulted from the computational errors.

5.3 Damage Localization

Damage localization results for the selected damage detection algorithms are presented in Figures 3-8. It is obvious from Figures 3(a) and 3(b) that the small size damage can not be localized accurately in presence of temperature effect using FBDD method. The effect of temperature on damage localization is more prominent when this small size damage is located away from the midspan. However, all size of damage can be localized accurately [Figure 3(c)] even in presence of temperature effect when the damage is located very close to midspan. The absolute

Table 3: MAC values for the intact and the damaged (case C9) displacement mode shapes

Damaged beam	Intact beam				
	1	2	3	4	5
1	1	3.8×10^{-7}	6.8×10^{-9}	3.3×10^{-8}	5.2×10^{-9}
2	3.8×10^{-7}	1	1.1×10^{-7}	4.4×10^{-7}	6.1×10^{-8}
3	6.8×10^{-9}	1.1×10^{-7}	1	4.3×10^{-7}	3.2×10^{-8}
4	3.3×10^{-8}	4.4×10^{-7}	4.3×10^{-7}	1	1.8×10^{-5}
5	5.2×10^{-9}	6.1×10^{-8}	3.2×10^{-8}	1.8×10^{-5}	0.99

Table 4: MAC values for the intact and the damaged (case C10) displacement mode shapes

Damaged beam	Intact				
	1	2	3	4	5
1	1	3.8×10^{-7}	1.7×10^{-9}	2.4×10^{-8}	1.3×10^{-9}
2	3.8×10^{-7}	1	1.1×10^{-7}	5.1×10^{-7}	7.3×10^{-8}
3	1.7×10^{-9}	1.1×10^{-7}	0.99	4.2×10^{-7}	3.3×10^{-8}
4	2.4×10^{-8}	5.1×10^{-7}	4.2×10^{-7}	1	4.2×10^{-5}
5	1.3×10^{-9}	7.3×10^{-8}	3.3×10^{-8}	4.2×10^{-5}	0.99

difference between the mode shape curvatures of the intact and damage cases for the first five modes for different damage scenarios are plotted in Figure 4. It is obvious from the plot that the changes in MSC are highly localized to the damage inflicted regions, element 8, element 12 and element 16 in Figures 4(a), 4(b) and 4(c) respectively, for all damage cases. Similar results were obtained by applying the damage index method (Figure 5).

Flexibility change obtained from five vibration modes are plotted in Figure 6. Damage inflicted elements at different locations along the beam can be detected accurately for all levels of applied damage when the beam is not affected by the temperature change. As demonstrated in Figures 6(a) and 6(b), small size damage can not be detected accurately in presence of temperature effect when the damage inflicted element is located away from the midspan. In such conditions, maximum flexibility change was observed around midspan. At low damage levels, the change in flexibility due to temperature effect may be more significant than that due to a local change, which may cause the maximum change in flexibility around midspan. The plots of change in flexibility curvature for the studied damage scenarios are shown in Figure 7. Damages are clearly localized in all cases and the effect of the tem-

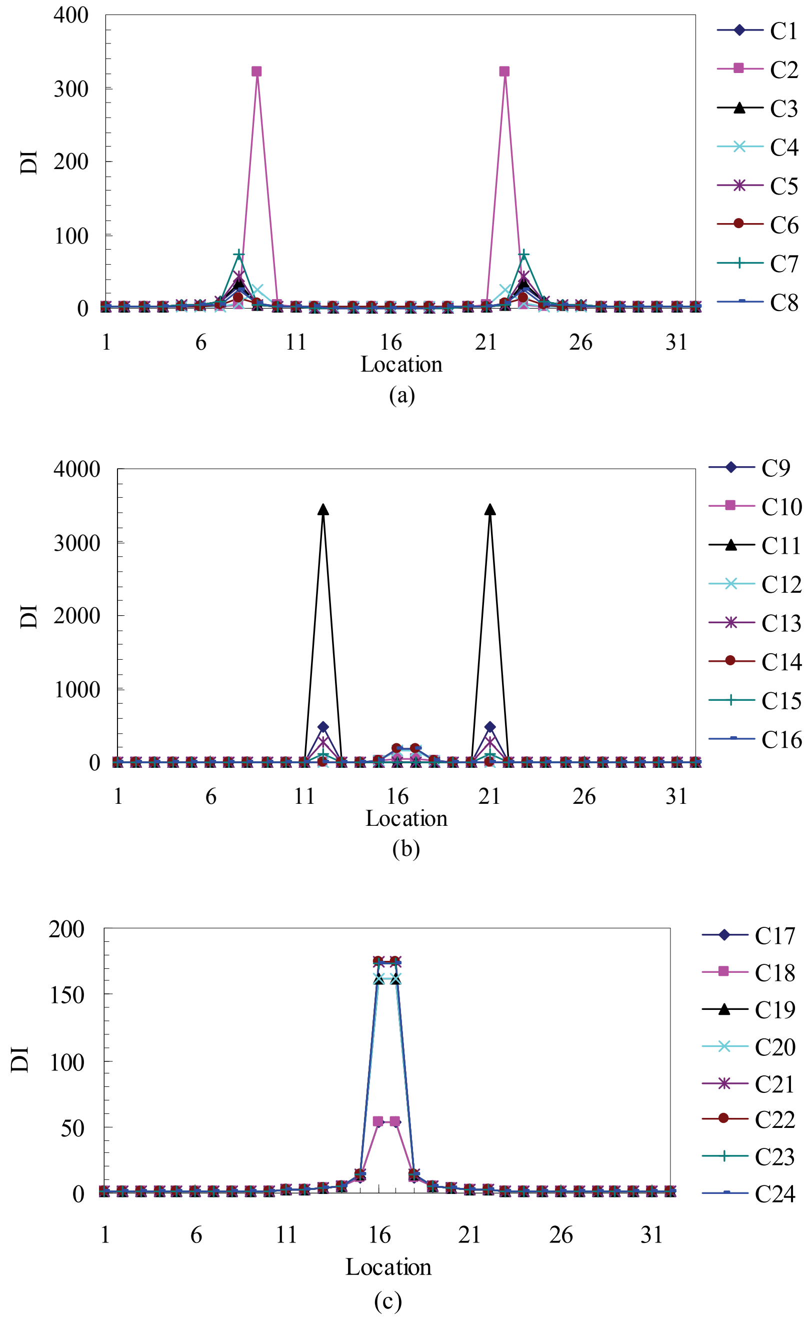

Figure 3: Frequency based damage identification method (a) damage at element 8 (b) damage at element 12 (c) damage at element 16

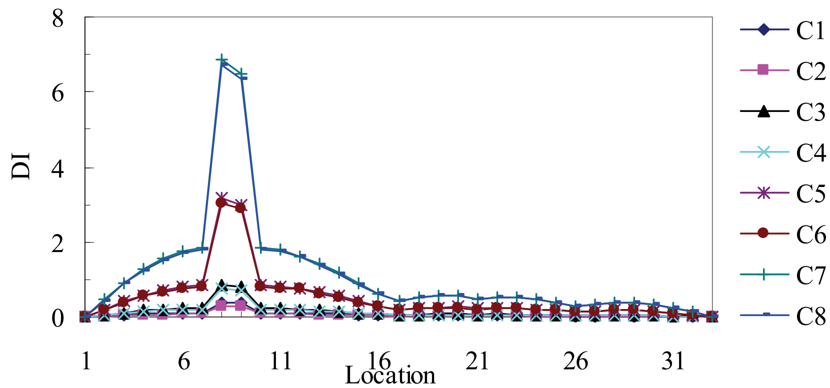

(a)

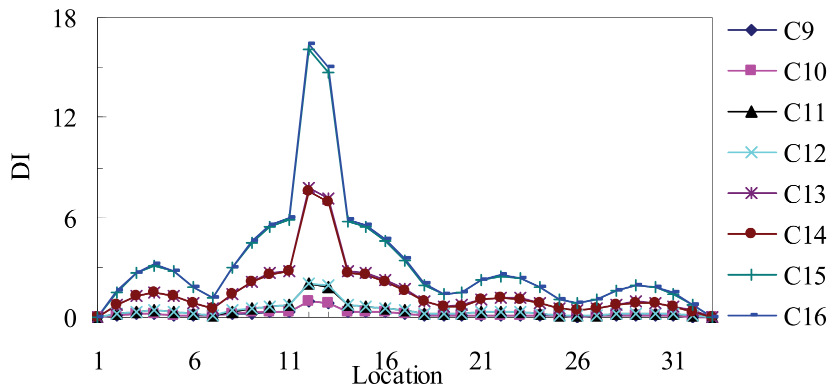

(b)

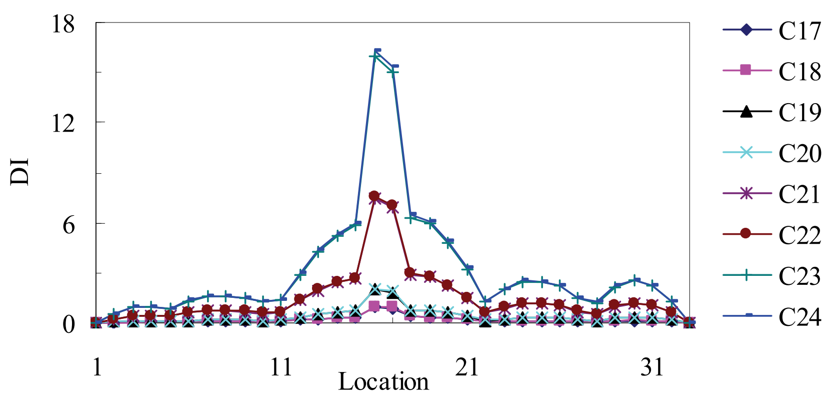

(c)

Figure 4: Mode shape curvature method (a) damage at element 8 (b) damage at element 12 (c) damage at element 16

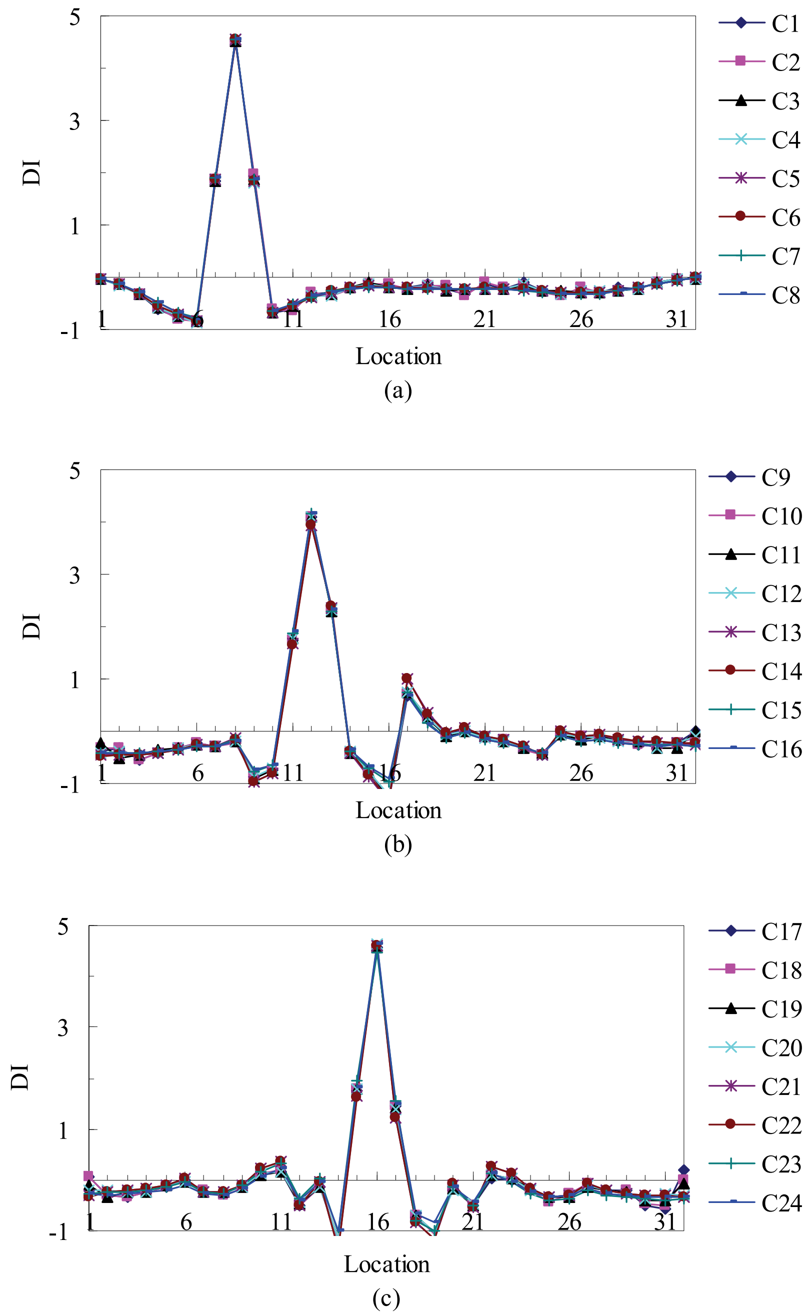

Figure 5: Mode shape curvature DI method (a) damage at element 8 (b) damage at element 12 (c) damage at element 16

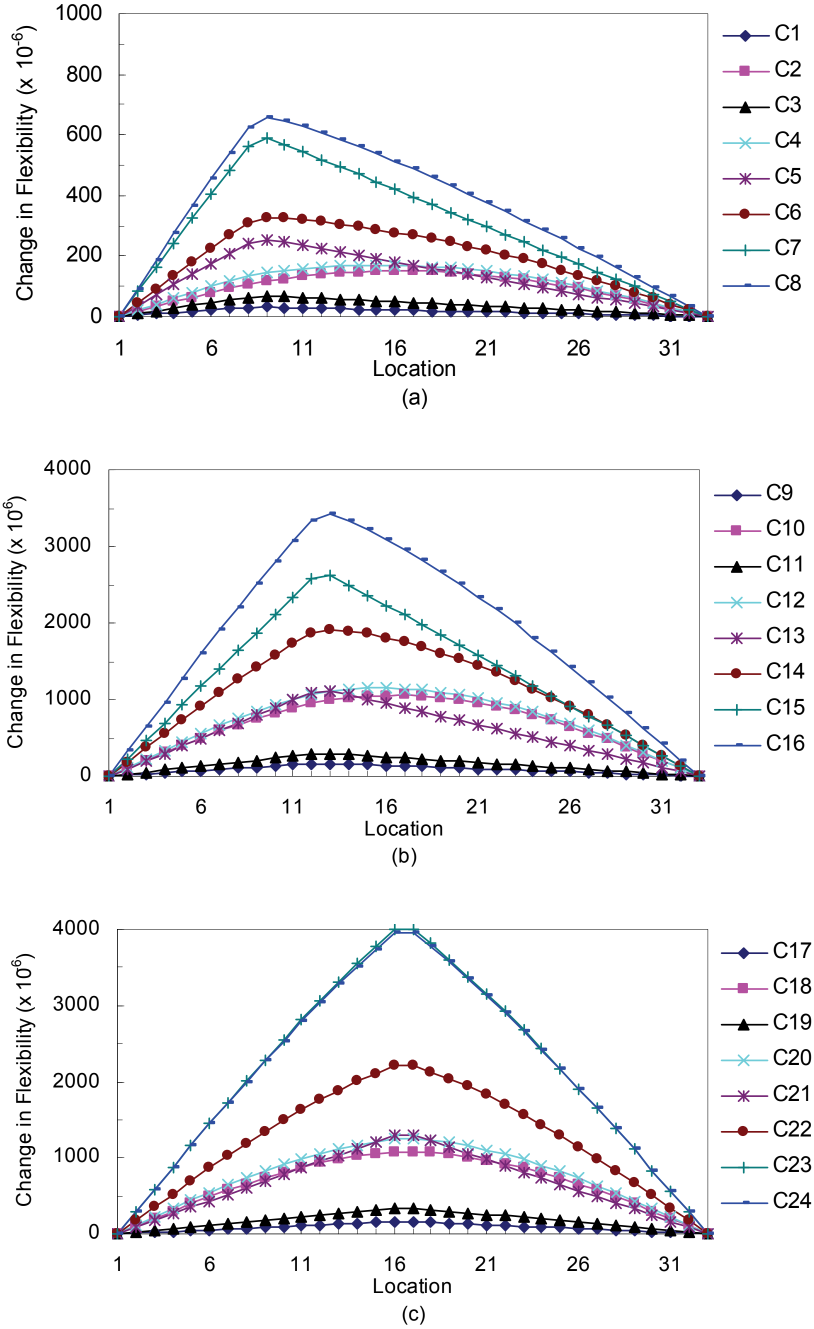

Figure 6: Change in flexibility method (a) damage at element 8 (b) damage at element 12 (c) damage at element 16

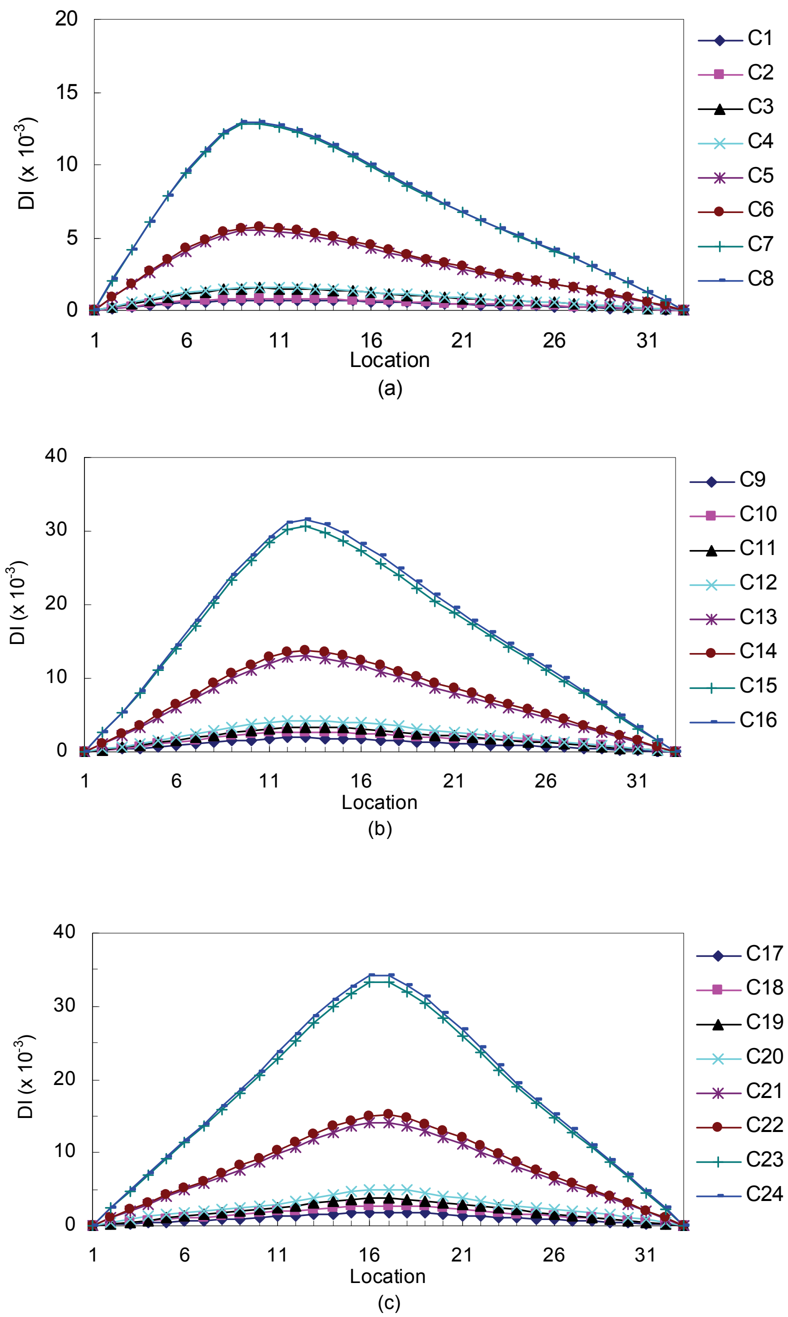

Figure 7: Change in flexibility curvature method (a) damage at element 8 (b) damage at element 12 (c) damage at element 16

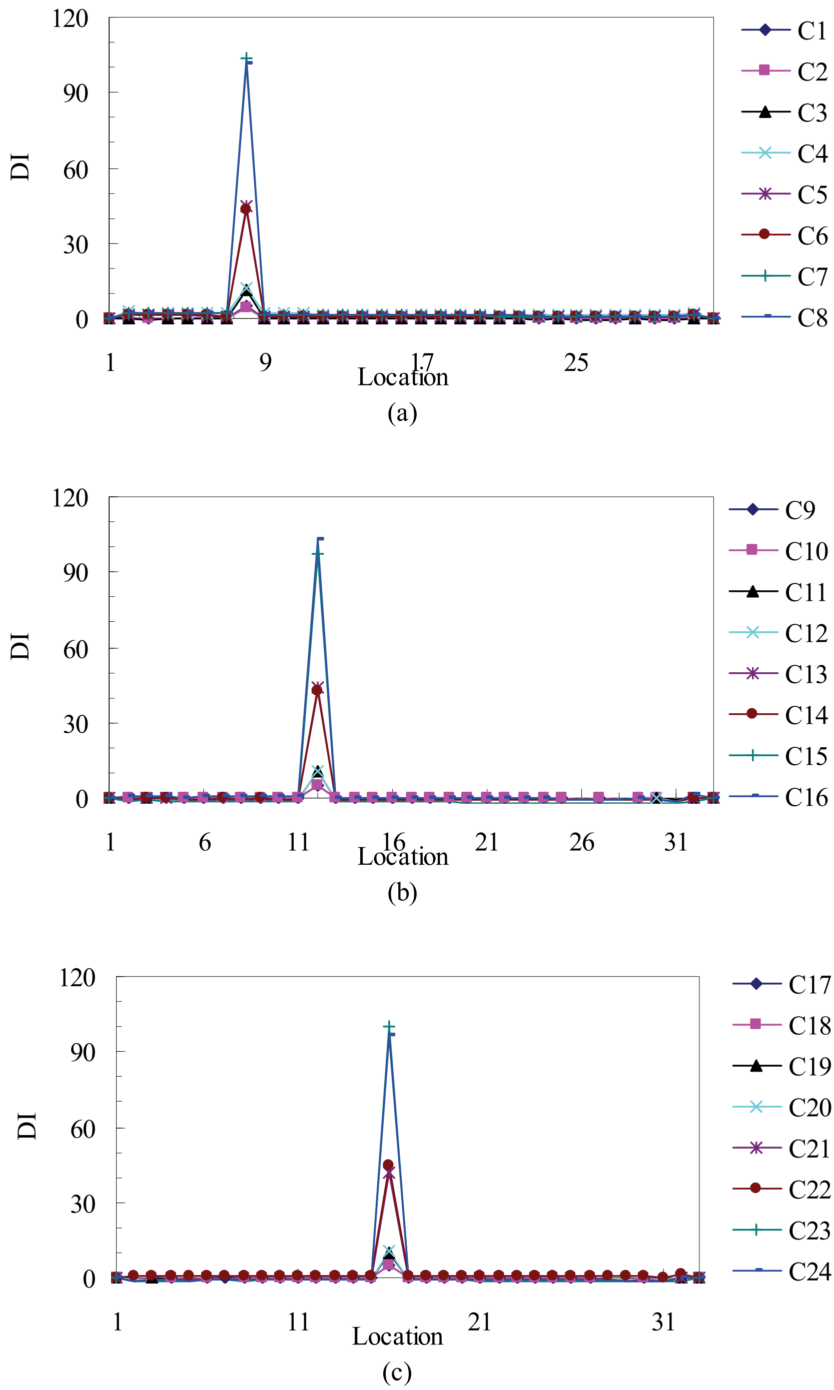

Figure 8: MMSV based DI method (a) damage at element 8 (b) damage at element 12 (c) damage at element 16

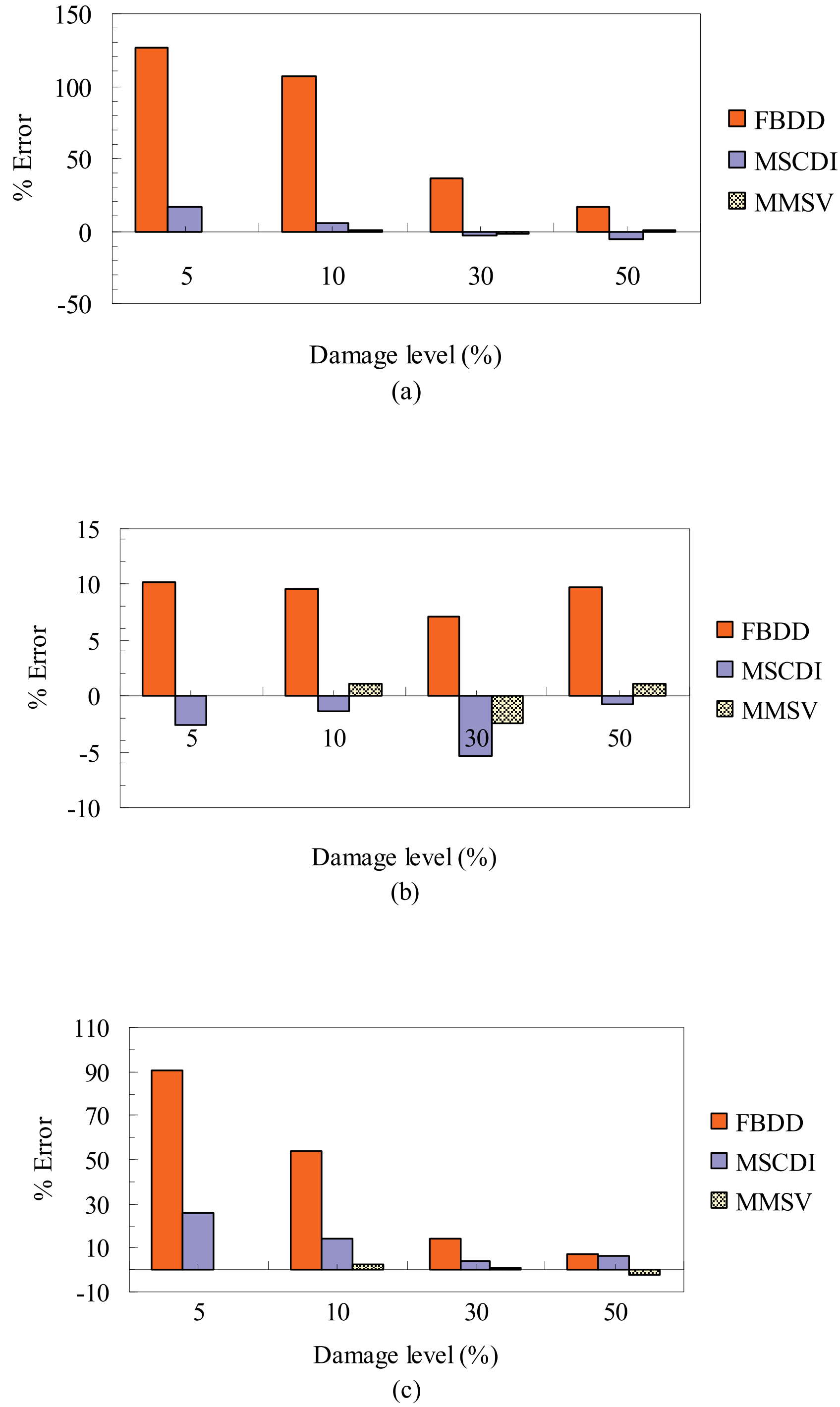

Figure 9: Percentage errors on damage quantification due to temperature effect (a) damage at element 8 (b) damage at element 12 (c) damage at element 16

perature on the calculated damage indices can be visually distinguished from this method.

MMSV based damage localization results are presented in Figure 8. Proper location of the damaged element can be clearly identified from the maximum value of the MMSV based damage index. Figure 8 distinctly shows that damage localization process is not affected by the influence of the temperature effect for all damage levels considered in this study.

5.4 Damage Quantification

The effect of temperature on damage quantification, denoted as percentage error, was obtained using the following equation

$$\%Error = 100x\frac{(\eta_T - \eta)}{\eta} \tag{20}$$

where η and η_T are the damage quantification results obtained without and with temperature effects, respectively. Percentage error on damage quantification due to temperature effect is plotted in Figure 9. It is obvious from Figure 9 that the damage quantification results in most cases are affected by the temperature effect. Among the selected algorithms, FBDD method is the most affected by the temperature effect. Maximum effect of the temperature change was observed for the damaged element 8 with 5% reduction in stiffness. For this case, the quantification error was computed as about 140% for 1% change in elastic modulus due to temperature effect. It can also be seen from Figure 9 that quantified damage considering the temperature effect from FBDD method is always larger than that computed under constant temperature. This result is very similar to the change in frequency of the damaged beam with the application of temperature effect. However, this trend was not observed in other algorithms. Among the studied methods, MMSV based damage index method shows the least sensitivity to temperature effect in damage quantification.

6 Conclusions

The purpose of the paper is to illustrate the effect of environmental temperature on damage identification using the commonly used vibration-based damage identification techniques. Temperature can affect the structure in several ways. Effect on the elastic modulus of the material is considered to be the most responsible for changing the structure modal properties such as modal frequency. Through the numerical study it was also found that the variation of elastic modulus with temperature is much more significant than thermal expansion to alter the modal frequency. Simulation results show that temperature alone can cause a significant change in natural frequency of the intact structure for all modes. In some cases, drop in natural frequencies of the intact structure due to temperature effect can be higher than that caused by local structural damage. For damaged structure, temperature effect can magnify the drop in natural frequency significantly at low damage level. At high damage level, structural damage plays the vital role to alter the natural frequency of the structure. However, the mode shapes are not much affected by the variation of temperature. MAC values were computed to confirm the identicalness of the modes and were found almost equal to unity for every mode.

It is apparent from the simulation results that the selected vibration based damage identification methods distinctly localize damage for all damage scenarios at constant temperature. However, for some algorithms (FBDD and change in flexibility) temperature effect badly affects the localization process especially at low damage level and when the damage inflicted element is away from the midspan of the beam. This indicates that at low damage level the sensitivity to the temperature variation in damage localization depends also on the damage location. The problem in damage localization at low damage level due to the temperature variation may be due to the substantial change in stiffness of the whole beam caused by temperature effect compared to the reduction in stiffness of a single element due to structural damage. Since temperature effect has no significant influence on mode shapes, other algorithms can localize the low level damage considering the temperature effect. FBDD method also found to be the least efficient to quantify damage when temperature effect was applied. According to simulation results, temperature effect on damage quantification is also spatially related. Among the studied methods, MMSV based damage index method showed the best damage quantification.

References

Baldwin, R.; North, M.A. (1978): A stress–strain relationship for concrete at high temperatures. In: Concrete BRE building research series vol. 1: Practical studies from the building research establishment, The Construction Press, New York, pp. 171-175.

Brockenbrough, R.L.; Merritt, F.S. (1994): Structural steel designer's handbook, 2^{nd} ed. McGraw-Hill, New York.

Clough, R.W.; Penzien, J. (1993): Dynamics of structure, 2nd ed., McGraw-Hill, New York.

Cornwell, P.J.; Farrar, C.R.; Doebling, S.W.; Sohn, H. (1999): Environmental variability of modal properties, *Experimental Techniques,* vol. 23(6), pp. 45-58

Doebling, S.W., Farrar, C.R., Prime, M.B.; Shevitz, D.W. (1996): Damage identification and health monitoring of structural and mechanical systems from changes in their vibration characteristics: A literature review, Los Alamos National Laboratory Report, LA-13070-MS.

Ewins, D.J. (2000): *Modal testing—Theory, practice and application*, Research Studies Press Ltd, Baldock, Hertfordshire, UK.

Kim, J.T.; Ryu, Y.S.; Cho, H.M.; Stubbs, N. (2003): Damage identification in beam-type structures: frequency-based method vs mode-shape based method, *Engineering Structures,* vol. 25, pp. 57-67.

Li, S.Z.and Wu, Z.S. (2007). A non-baseline algorithm for damage locating in flexural structures using dynamic distributed macro-strain responses, *Earthquake Engineering and Structural Dynamics,* vol. 36(9), pp.1109-1125.

Lloyd, G.M.; Wang, M.L; Singh,V. (2000): Observed variations of mode frequencies of a prestressed concrete bridge with temperature, *Condition Monitoring of Materials and Structures Engineering Mechanics Conf. (EM2000)*, Austin, Tx-US, pp.179-189.

Montalovao, D.; Maia, N.M.M.; Riberio, A.M.R. (2006): A review of vibration-based structural health monitoring with special emphasis on composite materials, *The Shock and Vibration Digest,* vol. 38(4), pp. 295-324.

Pandey, A.K.; Biswas, M.; Samman, M.M. (1991): Damage detection from changes in curvature mode shapes, *Sound and Vibration,* vol.145(2), pp.321–332.

Pandey, A.K.; Biswas, M.(1994): Damage detection in structures using changes in flexibility, *Sound and Vibration*, vol. 69(1), pp.3–17.

Stubbs, N.; Kim, J.T.; Farrar, C.R. (1995): Field verification of a non-destructive damage localization and severity estimation algorithm, *13th International Modal Analysis Conference,* Nashville, USA, pp.210-218.

Wahab, M.A.; De Roeck, G. (1997): Effect of temperature on dynamic system parameters of a highway bridge, *Structural Engineering International*, vol.7(4), pp.266-270.

Xia, Y.; Hao, H.; Zanardo, G.; Deeks, A. (2006): Long term vibration monitoring of an RC slab: temperature and humidity effect, *Journal of Engineering Structures,* 28, 441-452.

Yan, A.M.; Kerschen, G.; De Boe, P; Golinval, J.C. (2005): Structural damage diagnosis under varying environmental conditions—Part I: A linear analysis, *Mechanical Systems and Signal Processing,* vol.19, pp. 847–864

Zhang, Z.; Aktan, A.E. (1995): The damage indices for constructed facilities, *13th International Modal Analysis Conference,* Nashville, USA, pp.1520-1529.